RESEARCH ARTICLE

Synthesis of closed-Heterohelicenes Interconvertible between Its Monomeric and Dimeric Forms

Yusuke Matsuo[a,b], Chihiro Maeda[c], Yusuke Tsutsui,[b,d] Takayuki Tanaka*[a,b], Shu Seki[b]

[a] Y. Matsuo, Dr. T. Tanaka
Department of Chemistry, Graduate School of Science, Kyoto University, Sakyo-ku, Kyoto 606-8502 (Japan)
[b] Y. Matsuo, Dr. Y. Tsutsui, Dr. T. Tanaka, Prof. Dr. S. Seki
Department of Molecular Engineering, Graduate School of Engineering, Kyoto University, Nishikyo-ku, Kyoto 615-8510 (Japan)
E-mail: tanaka@moleng.kyoto-u.ac.jp
[c] Dr. C. Maeda
Division of Applied Chemistry, Graduate School of Natural Science and Technology, Okayama University, Tsushima, Okayama 700-8530 (Japan)
[d] Dr. Y. Tsusui
JST-PRESTO, 4-1-8 Honcho, Kawaguchi, Saitama 332-0012 (Japan)

Abstract: *Oxidative fusion reaction of cyclic heteroaromatic pentads consisting of pyrrole and thiophene gave closed-heterohelicene monomers and dimers depending on the oxidation conditions. Specifically, oxidation with [bis(trifluoroacetoxy)iodo]benzene (PIFA) gave closed-[7]helicene dimers connected at the β-position of one of the pyrrole units with the remarkably elongated C–C bonds about 1.60 Å. Although this bond was intact against thermal and physical activations, homolytic bond dissociation took place upon UV irradiation in DMSO to give the corresponding monomers. Thus, interconversion between the closed-helicene monomer and dimer was achieved. The optically pure dimer was photo-dissociated into the monomers associated with circularly polarized luminescence (CPL) turn-ON.*

Introduction

Helicenes are polycyclic aromatic compounds with non-planar screw-shaped skeletons consisting of *ortho*-fused benzenes or other (hetero)aromatic rings.[1] Among intriguing physical and chemical properties of helicene-like molecules, primary interests have been given to inherently chiral topology which provides unique properties such as circular dichroism (CD) and circularly polarized luminescence (CPL). In particular, CPL materials are expected to be used as advanced optical information processing applications such as 3D displays, security paints, and optical communications.[2] In recent years, controlling the chiroptical properties of helicenes by external stimuli has been extensively studied by means of photoirradiation,[3] redox reaction,[4] and pH control.[5] In most of these studies, helicenes are equipped with some functional attachments that can respond to the stimuli. On the other hand, more smart materials in which the helicene backbone itself changes the structure upon external stimuli are quite rare.[6,7] In such a case, their chiroptical properties would be drastically affected in response to the structural changes.

Among functional helicene-like molecules, heteroatom-doped helicenes, hereafter called as heterohelicenes,[8-10] are attractive π-conjugated systems for helicene-based chiroptical molecular switches because of i) their emissive properties usually superior to carbohelicenes and ii) stimuli-responsibility at the heteroaromatic sites such as pyrrole, thiophene, and pyridine. For example, Champagne and Audisio have recently reported pH-responsive azahelicene **1**, in which the pyridyl unit embedded in the helical π-system was (de)protonated to cause reversal of the CPL sign (Figure 1a).[6a] Fuchter *et al.* reported redox-triggered reversible dimerization of azoniahelicene **2⁺**.[7] In this report, electrochemical reduction of **2⁺** gives its dimer $\mathbf{2_2}$, and this dimer can be converted back to **2⁺** upon oxidation. This is the first observation of a helicene-based redox interconversion between its monomer and dimer, although the exact structure of the dimer has not been elucidated in detail.

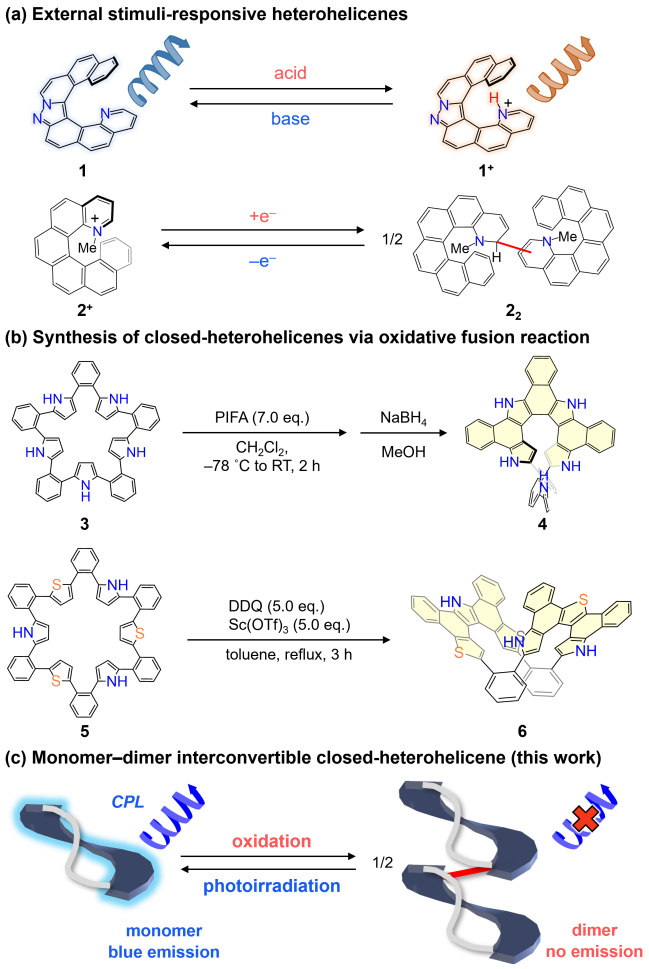

Figure 1. a) Examples of external stimuli-responsive heterohelicenes. b) Synthesis of closed-heterohelicenes by oxidative fusion reactions of cyclic

oligoarenes. c) Schematic representation for monomer–dimer interconversion of closed-helicenes (this work).

Recently, Tanaka and co-workers have reported a new synthetic strategy for closed-heterohelicenes in which the two ends of helicene are connected via a bridge segment.[11-14] For instance, the oxidative fusion reaction of *ortho*-phenylene-bridged cyclic hexapyrrole gave pentaaza[9]helicene with a diphenylpyrrole bridging segment.[12] When the number of constituted pyrrole units was reduced, cyclic pentapyrrole **3** showed different outcomes depending on the oxidation conditions. Namely, oxidation of **3** by [bis(trifluoroacetoxy)iodo]benzene (PIFA) at low temperature selectively gave closed-tetraaza[7]helicene **4**, while pentabenzopentaaza[10]circulene, a fully fused saddle-distorted heteronanographene, was obtained by oxidation with 2,3-dichloro-5,6-dicyano-1,4-benzoquinone (DDQ)/Sc(OTf)$_3$ under heating (Figure 1b).[13,14] In another case, [2,2]helicenophane **6** was synthesized exclusively from *ortho*-phenylene-bridged cyclic tripyrrole-trithiophene **5**.[15] As seen in these transformations, both the number of heteroaromatic units and the type of heteroatoms are crucial to the reaction, which drove us to examine the oxidation outcome from cyclic pentads consisting of pyrrole and thiophene. To our surprise, core-connected dimers of closed-hetero[7]helicenes were obtained, which, upon photoirradiation, dissociated into their monomers (Figure 1c). Herein, we report the details of the synthesis, structures, (chir)optical properties, and switching behavior of this unique closed-heterohelicene system.

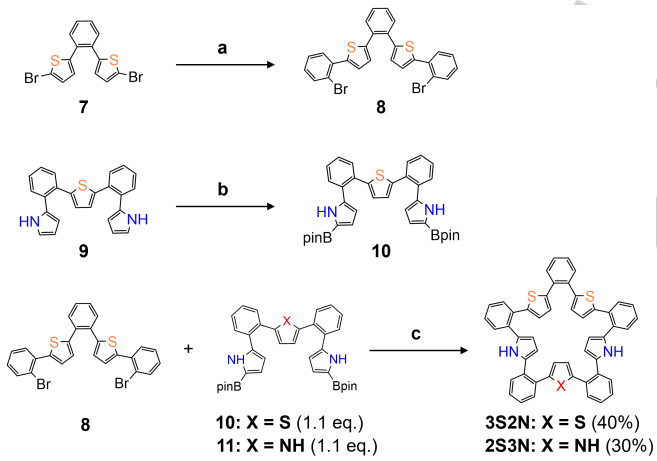

Scheme 1. Synthesis of *ortho*-phenylene-bridged cyclic pyrrole–thiophene hybrids **3S2N** and **2S3N**. a) 2-bromophenylboronic acid (2.2 eq.), Pd(PPh$_3$)$_4$ (5.0 mol%), Na$_2$CO$_3$ (10 eq.), 1,4-dioxane/H$_2$O, 90 ˚C, 24 h, yield: 88%. b) [Ir(cod)OMe]$_2$ (1.5 mol%), DTBPY (3.5 mol%), B$_2$pin$_2$ (1.2 eq.), THF, reflux, 12 h, yield: 60%. c) XPhos Pd G2 (5.0 mol%), K$_3$PO$_4$ (18 eq.), THF/H$_2$O, RT, 12 h. (cod =1,5-cyclooctadiene, DTBPY = 4,4'-di-*tert*-butyl-2,2'-dipyridyl.)

Results and Discussion

At first, we aimed at the synthesis of cyclic pyrrole–thiophene hybrid pentads in a [2+3] manner motivated by our successful synthesis of cyclic pentapyrrole as a precursor of pentabenzopentaaza[10]circulene.[14] 1,2-Bis(5-bromothien-2-yl)-benzene (**7**) was coupled with 2.2 equivalents of 2-bromophenyl-boronic acid to give a dibromo precursor, **8**, in 88% yield (Scheme 1). Its coupling partner **10** was synthesized by Ir-catalyzed borylation of **9** in 60% yield. Then, cross-coupling reaction of **8** with 1.1 equivalents of **10** or tripyrrole **11**[14] in the presence of 5.0 mol% XPhos Pd G2 and an excess amount of tripotassium phosphate gave **3S2N** and **2S3N** in 40% and 30% yields, respectively. The ^{1}H NMR spectra of **3S2N** and **2S3N** reflect their two-fold symmetry, which indicates that the conformational dynamics are much faster than the NMR timescale (Figure S3-5, 3-13). Single crystals suitable for X-ray diffraction (XRD) analysis were obtained by slow diffusion of *n*-hexane into their dichloro-methane solutions and the structures have been revealed by XRD analysis.[16] In the solid state, **3S2N** and **2S3N** take highly twisted conformations with average dihedral angles of 48.9˚ and 45.2˚, respectively between 1,2-phenylene bridges and pyrrole or thiophene rings (Figure S5-1, 5-4).

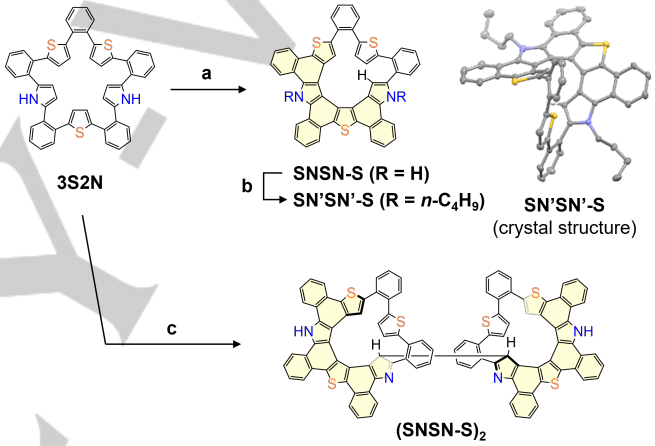

Scheme 2. Synthesis of closed-dithiadiaza[7]helicene monomers **SNSN-S**, **SN'SN'-S**, and dimer **(SNSN-S)$_2$**. a) FeCl$_3$ (15 eq.), CH$_2$Cl$_2$/MeNO$_2$, RT, 2 h, yield: 71%. b) 1-iodobutane (50 eq.), NaH (50 eq.), DMSO, 50 °C, 24 h, yield: 73%. c) i) PIFA (10 eq.), CH$_2$Cl$_2$, –78 ˚C to RT, 2 h, ii) NaBH$_4$ (excess), MeOH, RT, 10 min, yield: 51%. (PIFA = [bis(trifluoroacetoxy)iodo]benzene)

Next, oxidative fusion reaction of **3S2N** was attempted with iron(III) chloride at room temperature. After quenching with methanol, closed-dithiadiaza[7]helicene, **SNSN-S**, was obtained in 71% yield (Scheme 2). The structure was confirmed by ^{1}H NMR spectra and high-resolution atmospheric-pressure-chemical-ionization time-of-flight (HR-APCI-TOF) mass spectrometry (Figure S3-7 and S4-4). Although single crystals suitable for the XRD measurement were not obtained because of its low solubility, its *N*-butyl-substituted derivative, **SN'SN'-S**, was synthesized and analyzed by XRD measurement (Figure S5-2). The average dihedral angle of **SN'SN'-S** is 15.02° and the shortest and longest helical pitches are 3.435 Å ($C_\beta^{thiophene}$–$C_\beta^{pyrrole}$) and 4.877 Å ($C_\alpha^{thiophene}$–$C_\alpha^{pyrrole}$), respectively (Figure S5-10).[17] When PIFA was used as an oxidant and the reaction was quenched with sodium borohydride/methanol (NaBH$_4$/MeOH),[18,19] surprisingly, a dimeric product, **(SNSN-S)$_2$**, was obtained in 51% yield. Its HR-APCI-TOF-MS peaks were observed at *m/z* = 1499.2429 (calcd. for $C_{100}H_{50}N_4S_6$: *m/z* = 1499.2432). The structure of **(SNSN-S)$_2$** has been unambiguously revealed by XRD analysis (Figure 2).

Two [7]helicene backbones and thiophene linkers are located parallel and the π-π interactions are effective in both moieties. As a result of π-π interactions and steric hindrance of thiophene linkers, an unprecedented dimeric structure was obtained as stacked two helicenes interlocked by a C–C single bond. Notably, one of the pyrrolic amine-type nitrogen became imine-type one as judged from the bond lengths of C4–N1 (1.416(5) Å) and C5–N1 (1.278(5) Å). The C1–C2 bond connecting two helicenes was quite longer (1.596(7) Å) than usual C(sp^3)–C(sp^3) bond lengths. The C1–C5 bond (1.544(5) Å) and C1–C3 bond (1.538(6) Å) indicate that C1 is an sp^3-carbon, the spectrum of which is observed by ^{13}C NMR measurement in DMSO-d_6 at 53.8 ppm (Figure S3-10). The configurations of two helicene moieties have been assigned as (*P*,*P*) or (*M*,*M*) (*vide infra*).[20] The helical pitches are 3.572 and 3.646 Å ($C_\beta^{thiophene}$–$C_\beta^{pyrrole}$) and 5.057 and 5.200 Å ($C_\alpha^{thiophene}$–$C_\alpha^{pyrrole}$) (Figure S5-10).[13] Production of the corresponding *meso*-isomer, (*P*,*M*)-**(SNSN-S)$_2$**, is unlikely feasible due to steric constraints between two helicene units.

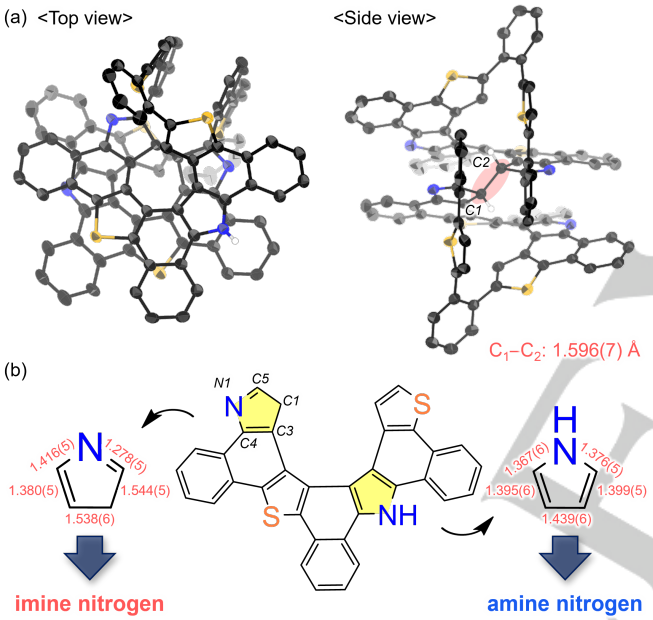

Figure 2. a) X-Ray crystal structure of **(SNSN-S)$_2$** with thermal ellipsoids at 50% probability. (Left) Top view and (right) side view. Solvent molecules and hydrogen atoms except for two C(sp^3)–Hs have been omitted for clarity. b) Selected bond lengths (Å).

This dimer **(SNSN-S)$_2$** was not obtained by the use of other oxidants such as DDQ/Sc(OTf)$_3$ or tris(4-bromophenyl)-ammoniumylhexachloroantimonate (Magic blue), and monomer **SNSN-S** was mainly obtained instead (Table S2-1, S2-2). When the oxidation with PIFA was conducted with **SNSN-S** as a substrate, **(SNSN-S)$_2$** was obtained in 82% yield. However, the same reaction with *N*-butyl derivative **SN'SN'-S** did not furnish dimerization. These results suggest that dimerization of this helicene does not proceed by a simple pathway via radical cation species, and the free NH sites of the pyrrole units play an important role in dimerization. Recently, *N*-iodine(III) species of indole has been reported as an electrophilic indole surrogate via umpolung with hypoiodite catalysis.[21] In the present dimerization, a similar *N*-iodine(III) intermediate can be thought to be involved (Figure S7-16). Under this hypothesis, $NaBH_4$ also plays a role in reducing products excessively oxidized by PIFA.[22] In the case of **2S3N**, the same protocol with PIFA and $NaBH_4$/MeOH can be adopted to give dimer **(SNNN-S)$_2$** in 71% yield, while oxidation by other oxidants gave thiatriaza[7]helicene **SNNN-S** up to 19% isolated yield, again without any traces of dimeric products. The structure was confirmed, again after alkylation to afford **SN'N'N'-S** (Figure S5-5). Characterization of this dimer **(SNNN-S)$_2$** has been accomplished by XRD analysis to be an essentially the same dimeric structure as of **(SNSN-S)$_2$** (Figure S5-7 and S5-8). The C–C bond connecting two helicene cores is 1.602(3) Å, being slightly longer than that of **(SNSN-S)$_2$** (Figure S5-6). This is probably because **(SNNN-S)$_2$** contains two more electron-rich pyrrole units and π–π electrostatic repulsion between two helical cores would be larger than that of **(SNSN-S)$_2$**. The average dihedral angle of 14.29° and the shortest helical pitches ($C_\beta^{thiophene}$–$C_\beta^{pyrrole}$) of 3.383 Å are within the same range as of **(SNSN-S)$_2$** while the longest helical pitch becomes shorter (4.843 Å). The interactions among the two helicene moieties were visualized using the non-covalent interaction (NCI) analysis.[23] Accordingly, dispersion interactions between two stacked helicene units are obviously shown (Figure S7-18).

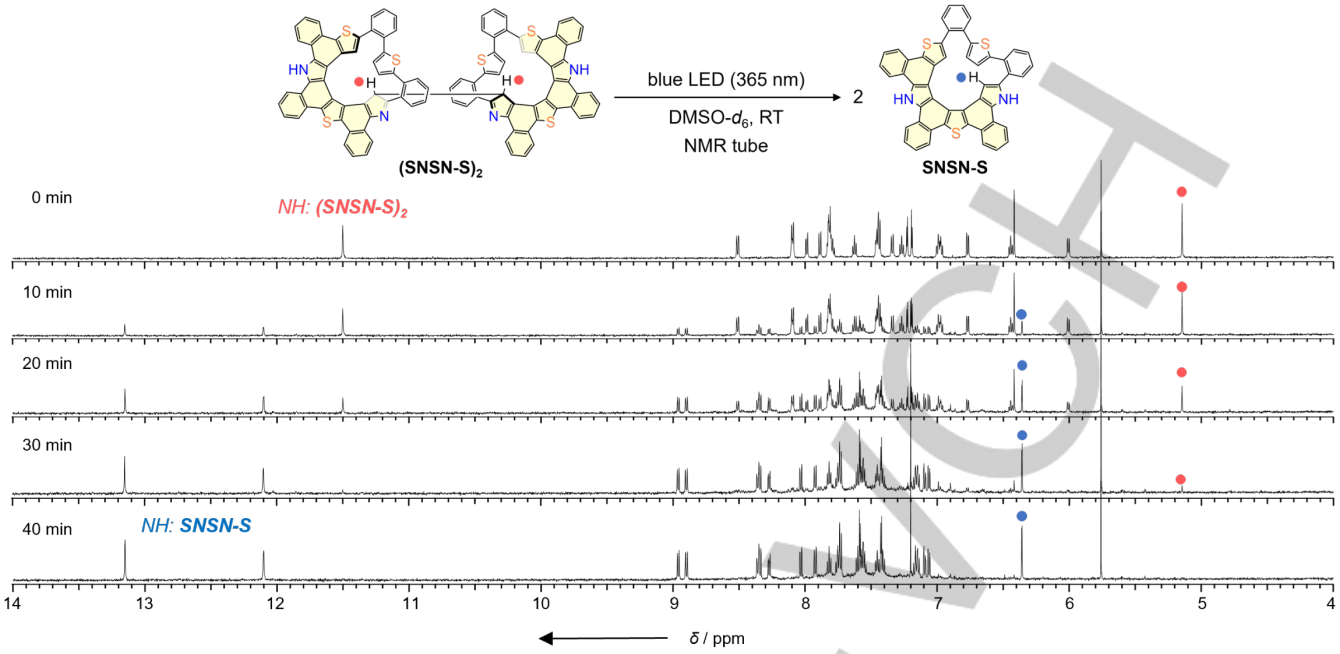

Figure 3. ^{1}H NMR spectral change of **(SNSN-S)$_2$** in DMSO-d_6 (1.1 x 10^{-3} M) at room temperature in open air upon photoirradiation (365 nm).

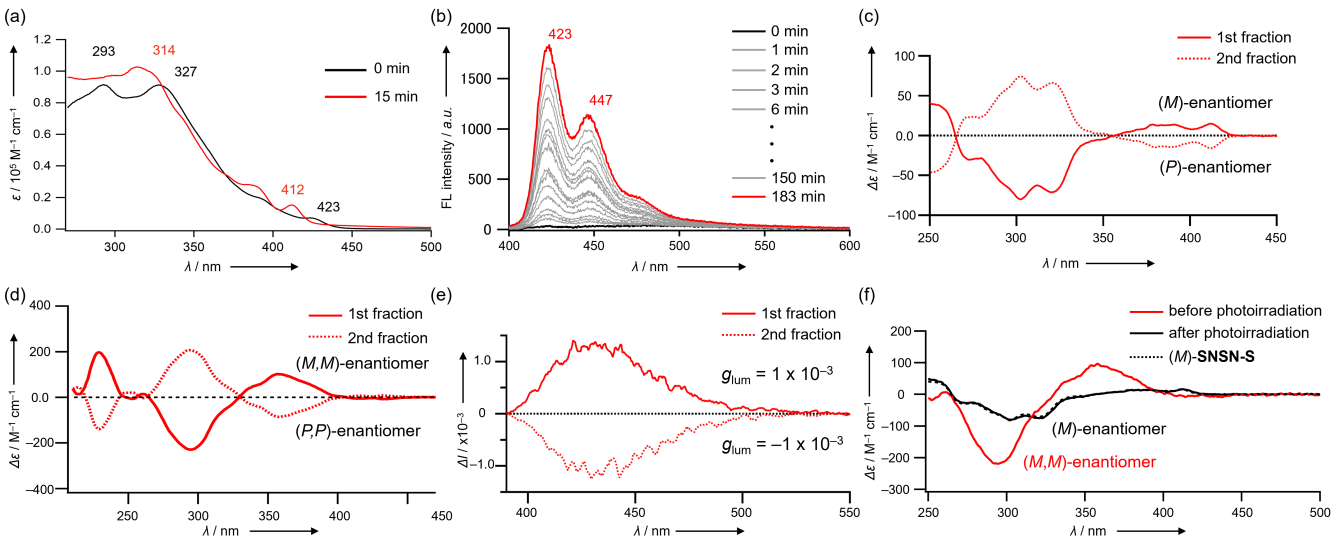

Figure 4. Absorption and fluorescence spectral changes of **(SNSN-S)$_2$** upon photoirradiation (365 nm) in THF. ([**(SNSN-S)$_2$**]$_0$ = 2 × 10^{-5} M for a) and 6 × 10^{-6} M for b). CD spectra of the enantiomerically pure c) **SNSN-S** and d) **(SNSN-S)$_2$** in THF. e) CPL spectra of **SNSN-S** in THF. f) CD spectral change before and after photoirradiation in THF.

UV/Vis absorption and fluorescence spectra were measured in THF. Cyclic pentad **3S2N** showed broad absorption and fluorescence bands, reflecting its conformational flexibility as observed in other cyclic hybrids (Figure S6-1).[12-14,24] On the other hand, **SNSN-S** exhibited structured absorption bands at 387 and 412 nm and sharp fluorescence bands with a vibronic structure at 422 and 446 nm. The fluorescence quantum yield is 0.03. **(SNSN-S)$_2$** showed a slightly red-shifted absorption spectrum and a very broad emission band with its quantum yield practically less than 0.001.

Although ^{1}H NMR spectra of **SNSN-S** and **(SNSN-S)$_2$** measured in DMSO-d_6 were indeed complicated reflecting their lower symmetry, the peaks corresponding to pyrrolic NHs were observed at 13.15 and 12.10 ppm for **SNSN-S** and 11.50 ppm for

(SNSN-S)$_2$. During our experiments, surprisingly, we observed that the peaks of **(SNSN-S)$_2$** gradually disappeared upon photoirradiation (Figure 3). Instead, monomer **SNSN-S** was produced almost quantitatively within 40 min. This conversion may be ascribed to the photodissociation of the long C–C bond to recover the aromaticity of the terminal pyrrole segment.[25,26] We also examined the bond activation by heating, mechanical force, and addition of strong acids. However, these stimuli were not as effective as photoirradiation, and only trace amount of **SNSN-S** was produced under heating at 140 °C in DMSO-d_6 for 3 days (Figure S3-22). The dissociation reaction can be conducted in a batch scale under blue light-emitting-diode (LED) (365 nm), and **SNSN-S** was obtained in 74% isolated yield. In a similar manner, the reaction of **(SNNN-S)$_2$** under photoirradiation gave **SNNN-S** in 52% isolated yield.

The C–C bond dissociation by photoirradiation was also followed by changes in the absorption spectra in THF (Figure 4a). In the concentration used for these measurements (ca. 10^{-5}), spectral changes saturated in about 15 minutes. With the more diluted solution (ca. 6×10^{-6} M), the fluorescence spectral changes were monitored with more detailed set-up (Figure 4b).[27] As the dissociation reaction proceeds, the emission is gradually enhanced, and the spectrum became almost identical to that of **SNSN-S** in THF (Figure S6-1). The plot of emission intensity detected at 423 nm versus irradiation time showed that the change saturated at approximately 180 minutes, with a time constant of 43.5 minutes (Figure S6-5). Time-dependent density-functional-theory (TD-DFT) calculations of **SNSN-S** and **(SNSN-S)$_2$** at TD-B3LYP/6-311G(d,p) level allowed us to assign the lowest energy absorption bands to be the highest-occupied-molecular orbital (HOMO) to the lowest-unoccupied-molecular-orbital (LUMO) excitations (**SNSN-S**: 401 nm, f = 0.0829) and the forbidden HOMO to LUMO transition (**(SNSN-S)$_2$**: 421 nm, f = 0.0037), being consistent with the gradual emission enhancement from dimer to monomer (Figure S7-9).

Finally, the twisted structures of heterohelicene monomer and dimer prompted us to examine their enantiomeric separation. Through screening of the chiral stationary phases and eluents, **SNSN-S** and **(SNSN-S)$_2$** were successfully separated into their enantiomers (Figure S9-1). The fundamental properties of the optically-resolved heterohelicenes (^{1}H NMR and HR-MS) were the same as those of the racemates. The CD spectra of them were measured, which displayed mirror-imaged spectra (Figure 4c,d). The absolute configuration was deduced by TD-DFT calculations (Figure S9-3). Only monomer **SNSN-S** showed clear mirror imaged CPL spectra, from which the g value of 1.2×10^{-3} was recorded (Figure 4e). This value is comparable to those reported for azahelicene-type molecules such as **1** and **1$^+$**.[6a] Retention of the chirality during the photodissociation from **(SNSN-S)$_2$** to **SNSN-S** was confirmed (Figure 4f). In a similar way, **SNNN-S**, and **(SNNN-S)$_2$** could also be optically resolved, yielding CD and CPL spectra (Figure S9-1, 9-2). However, due to the weaker emission of **SNNN-S** (Φ_F <0.01.) as compared with **SNSN-S**, the CPL spectra were not strong enough to calculate the g value. Finally, it is important to note that none of the obtained closed heterohelicenes enantiomerically purified in this study showed racemization at room temperature or even under heating in THF. Theoretical calculations at the B3LYP-D3(BJ)/def2-SVP level predicted that the racemization transition states are saddle-like structures whose inversion barriers at 298 K are significantly large (+48.8 kcal/mol for **SNSN-S** and +42.8 kcal/mol for **SNNN-S**) (Figure S9-4, S9-5).[28] In the case of **(SNSN-S)$_2$** and **(SNNN-S)$_2$**, the racemization activation barriers are expected to be even higher due to the greater steric constraints.

Conclusion

In conclusion, oxidative fusion of cyclic heteroaromatic pentads consisting of pyrrole and thiophene gave novel closed-heterohelicenes and, specifically, oxidation by PIFA gave double-layered heterohelicene dimers in good yields. From the XRD analysis, these closed-heterohelicenes displayed highly strained structures. More interestingly, dimers have an elongated C–C bond about 1.6 Å which connected two helicene cores, and photoirradiation to the dimers afforded monomers presumably via homolytic C–C bond dissociation. As only monomer exhibited blue emission and CPL, the enantiomerically pure dimer could be photodissociated into the corresponding enantiomer of emissive monomer, which demonstrated the availability as a turn-ON type CPL emitter. Studies on the synthesis and functionality of novel hetero-helicenes are actively ongoing in our group.

Acknowledgements

This work was supported by JSPS KAKENHI Grant Numbers (JP21H05480, JP22H00314, and JP23K17942). T.T. gratefully acknowledges the Foundation of the Promotion of Ion Engineering and the Asahi Glass Foundation for financial supports. Y. M. acknowledges a JSPS fellowship for young scientists.

Conflict of Interest

The authors declare no conflict of interest.

Keywords: nanographene • heterohelicene • oxidative fusion reaction • bond dissociation • circularly polarized luminescence

[1] a) R. H. Martin, *Angew. Chem. Int. Ed. Engl.* **1974**, *13*, 649; b) S. Grimme, J. Harren, A. Sobanski, F. Vögtle, *Eur. J. Org. Chem.* **1998**, 1491; c) A. Urbano, *Angew. Chem. Int. Ed.* **2003**, *42*, 3986; *Angew. Chem.* **2003**, *115*, 4116; d) S. K. Collins, M. P. Vachon, *Org. Biomol. Chem.* **2006**, *4*, 2518; e) Y. Shen, C. F. Chen, *Chem. Rev.* **2012**, *112*, 1463; f) M. Gingras, *Chem. Soc. Rev.* **2013**, *42*, 968; g) M. Gingras, G. Félix, R. Peresutti, *Chem. Soc. Rev.* **2013**, *42*, 1007; h) W.-L. Zhao, M. Li, H.-Y. Lu, C.-F. Chen, *Chem. Commun.* **2019**, *55*, 13793; i) K. Dhbaibi, L. Favereau, J. Crassous, *Chem. Rev.* **2019**, *119*, 8846; j) M. Jakubec, J. Storch, *J. Org. Chem.* **2020**, *85*, 13415; k) A. Tsurusaki, K. Kamikawa, *Chem. Lett.* **2021**, *50*, 1913; l) T. Mori, *Chem. Rev.* **2021**, *121*, 2373; m) P. Ravat, *Chem. Eur. J.* **2021**, *27*, 3957.

[2] a) I. Sato, R. Yamashima, K. Kadowaki, J. Yamamoto, T. Shibata, K. Soai, *Angew. Chem. Int. Ed.* **2001**, *40*, 1096; b) R. Hassey, E. J. Swain, N. I. Hammer, D. Venkataraman, M. D. Barnes, *Science* **2006**, *314*, 1437; c) G. Muller, *Dalton Trans.* **2009**, 9692; d) R. Farshchi, M. Ramsteiner, J. Herfort, A. Tahraoui, H. T. Grahn, *Appl. Phys. Lett.* **2011**, *98*, 162508; e)

Y. Yang, R. C. D. Costa, M. J. Fuchter, A. J. Campbell, *Nat. Photon.* **2013**, *7*, 634; f) F. Song, G. Wei, X. Jiang, F. Li, C. Zhu, Y. Cheng, *Chem. Commun.* **2013**, *49*, 5772; g) Y. Yang, R. C. D. Costa, D. M. Smilgies, A. J. Campbell, M. J. Fuchter, *Adv. Mater.* **2013**, *25*, 2624; h) V. Kiran, S. P. Mathew, S. R. Cohen, I. H. Delgado, J. Lacour, R. Naaman *Adv. Mater.* **2016**, *28*, 1957.

[3] a) T. B. Norsten, A. Peters, R. McDonald, M. Wang, N. R. Branda, *J. Am. Chem. Soc.* **2001**, *123*, 7447; b) Z. Y. Wang, E. K. Todd, X. S. Meng, J. P. Gao, *J. Am. Chem. Soc.* **2005**, *127*, 11552; c) T. J. Wigglesworth, D. Sud, T. B. Norsten, V. S. Lekhi, N. R. Branda, *J. Am. Chem. Soc.* **2005**, *127*, 7272; d) J. N. Moorthy, P. Venkatakrishnan, S. Sengupta, M. Baidya, *Org. Lett.* **2006**, *8,* 4891.

[4] a) J. K. Zak, M. Miyasaka, S. Rajca, M. Lapkowski, A. Rajca, *J. Am. Chem. Soc.* **2010**, *132*, 3246; b) E. Anger, M. Srebro, N. Vanthuyne, L. Toupet, S. Rigaut, C. Roussel, J. Autschbach, J. Crassous, R. Réau, *J. Am. Chem. Soc.* **2012**, *134*, 15628; c) T. Biet, A. Fihey, T. Cauchy, N. Vanthuyne, C. Roussel, J. Crassous, N. Avarvari, *Chem. Eur. J.* **2013**, *19*, 13160; d) D. Schweinfurth, M. Zalibera, M. Kathan, C. Shen, M. Mazzolini, N. Trapp, J. Crassous, G. Gescheidt, F. Diederich, *J. Am. Chem. Soc.* **2014**, *136*, 13045; e) M. Srebro, E. Anger, B. Moore II, N. Vanthuyne, C. Roussel, R. Réau, J. Autschbach, J. Crassous, *Chem. Eur. J.* **2015**, *21*, 17100.

[5] a) E. Anger, M. Srebro, N. Vanthuyne, C. Roussel, L. Toupet, J. Autschbach, R. Réau, J. Crassous, *Chem. Commun.* **2014**, *50*, 2854; b) N. Saleh, B. Moore, M. Srebro, N. Vanthuyne, L. Toupet, J. A. G. Williams, C. Roussel, K. K. Deol, G. Muller, J. Autschbach, J. Crassous, *Chem. Eur. J.* **2015**, *21*, 1673.

[6] a) E. Yen-Pon, F. Buttard, L. Frédéric, P. Thuéry, F. Taran, G. Pieters, P. A. Champagne, D. Audisio, *JACS Au* **2021**, *1*, 807; b) P. Karak, J. Choudhury, *Chem. Sci.* **2022**, *13*, 11163.

[7] J. R. Brandt, L. Pospíšil, L. Bednárová, R. C. da Costa, A. J. P. White, T. Mori, F. Teplý, M. J. Fuchter, *Chem. Commun.* **2017**, *53*, 9059.

[8] a) N. Takenaka, R. S. Sarangthem, B. Captain, *Angew. Chem. Int. Ed.* **2008**, *47*, 9708; *Angew. Chem.* **2008**, *120*, 9854; b) K. Goto, R. Yamaguchi, S. Hiroto, H. Ueno, T. Kawai, H. Shinokubo, *Angew. Chem. Int. Ed.* **2012**, *51*, 10333; *Angew. Chem.* **2012**, *124*, 10479; c) W. Hua, Z. Liu, L. Duan, G. Dong, Y. Qiu, B. Zhang, D. Cui, X. Tao, N. Cheng, Y. Liu, *RCS Adv.* **2015**, *5*, 75; d) T. Otani, A. Tsuyuki, T. Iwachi, S. Someya, K. Tateno, H. Kawai, T. Saito, K. S. Kanyiva, T. Shibata, *Angew. Chem. Int. Ed.* **2017**, *56*, 3906; *Angew. Chem.* **2017**, *129*, 3964; e) S. K. Pedersen, K. Eriksen, M. Pittelkow, *Angew. Chem. Int. Ed.* **2019**, *58*, 18419; *Angew. Chem.* **2019**, *131*, 18590; f) J. Feng, L. Wang, X. Xue, Z. Chao, B. Hong, Z. Gu, *Org. Lett.* **2021**, *23*, 8056; g) M. Salim, H. Ubukata, T. Kimura, M. Karikomi, *Tetrahedron Lett.* **2011**, *52*, 6591; h) T. Yanagi, T. Tanaka, H. Yorimitsu, *Chem. Sci.* **2021**, *12*, 2784; i) Y. Hashmi, T. Thongpanchang, *Eur. J. Org. Chem.*, **2023**, *26*, e202201373.

[9] a) A. Rajca, H. Wang, M. Pink, S. Rajca, *Angew. Chem. Int. Ed.* **2000**, *39*, 4481; *Angew. Chem.* **2000**, *112*, 4655; b) A. Rajca, M. Miyasaka, M. Pink, H. Wang, S. Rajca, *J. Am. Chem. Soc.* **2004**, *126*, 15211; c) C. Li, J. Shi, L. Xu, Y. Wang, Y. Cheng, H. Wang, *J. Org. Chem.* **2009**, *74*, 408; d) X. Liu, H. Sun, W. Xu, S. Wan, J. Shi, C. Li, H. Wang, *Org. Chem. Front.* **2018**, *5*, 1257; e) J. Wang, G. Wang, C. Li, Y. Dong, Z. Ma, H. Wang, *J. Org. Chem.* **2021**, *86*, 4413.

[10] a) K. Schickedanz, T. Trageser, M. Bolte, H.-W. Lerner, M. Wagner, *Chem. Commun.* **2015**, *51*, 15808; b) F. Miyamoto, S. Nakatsuka, K. Yamada, K.-i. Nakayama, T. Hatakeyama, *Org. Lett.* **2015**, *17*, 6158; c) T. Katayama, S. Nakatsuka, H. Hirai, N. Yasuda, J. Kumar, T. Kawai, T. Hatakeyama, *J. Am. Chem. Soc.* **2016**, *138*, 5210; d) S. Oda, B. Kawakami, Y. Yamasaki, R. Matsumoto, M. Yoshioka, D. Fukushima, S. Nakatsuka, T. Hatakeyama, *J. Am. Chem. Soc.*, **2022**, *144*, 106; e) D. Volland, J. Niedens, P. T. Geppert, M. J. Wildervanck, F. Full, A. Nowak-Król, *Angew. Chem. Int. Ed.* **2023**, *62*, e202304291; *Angew. Chem.* **2023**, *135*, e202304291.

[11] T. Tanaka, *Bull. Chem. Soc. Jpn.* **2022**, *95*, 602.

[12] F. Chen, T. Tanaka, Y. Hong, T. Mori, D. Kim, A. Osuka, *Angew. Chem. Int. Ed.* **2017**, *56*, 14688; *Angew. Chem.* **2017**, *129*, 14880.

[13] About hetero[n]circulenes; a) T. Hensel, N. N. Anderson, M. Plesner, M. Pittelkow, *Synlett* **2016**, *27*, 498; b) Y. Miyake, H. Shinokubo, *Chem. Commun.* **2020**, *56*, 15605; c) K. Kise, T. Tanaka, *Heterocycles* **2022**, *104*, 1373.

[14] Y. Matsuo, K. Kise, Y. Morimoto, A. Osuka, T. Tanaka, *Angew. Chem. Int. Ed.* **2022**, *61*, e202116789; *Angew. Chem.* **2022**, *134*, e202116789.

[15] Y. Matsuo, A. Osuka, T. Tanaka, *Synthesis* **2022**, *51*, 147.

[16] CCDC 2205273 (**3S2N**), 2205276 (**SN'SN'-S**), 2205277 (**(SNSN-S)$_2$**), 2205272 (**2S3N**), 2205275 (**SN'N'N'-S**), and 2205274 (**(SNNN-S)$_2$**) contain the supplementary crystallographic data for this paper. These data are provided free of charge by The Cambridge Crystallographic Data Centre.

[17] These pitches are longer than those of calculated structures without the diphenylthiophene linker. This implies that the presence of the linker indeed increases the strain energy. See Figure S7-14 (for monomer) and Figure S7-15 (for dimer) in the Supporting Information.

[18] F. Chen, T. Tanaka, T. Mori, A. Osuka, *Chem. Eur. J.* **2018**, *24*, 7489.

[19] Y. Matsuo, F. Chen, K. Kise, T. Tanaka, A. Osuka, *Chem. Sci.* **2019**, *10*, 11006.

[20] Because **(SNSN-S)$_2$** has two chiral sp^3 carbon atoms, the chirality definitions of (*R*,*R*) for (*P*,*P*)-**(SNSN-S)$_2$** and (*S*,*S*) for (*M*,*M*)-**(SNSN-S)$_2$** based on the Cahn-Ingold-Prelog rule can also be adopted.

[21] a) Y. Zhou, D. Li, S. Tang, H. Sun, J. Huang, Q. Zhu, *Org. Biomol. Chem.* **2018**, *16*, 2039; b) H. Tanaka, N. Ukegawa, M. Uyanik, K. Ishihara, *J. Am. Chem. Soc.* **2022**, *144*, 5756; c) Y. Zhu, S. Yang, E. Pu, L. Li, S. Ye, L. Wei, G. Ma, Y. Zhang, H. Zhang, J. Chen, *Org. Lett.* **2023**, *25*, 3533.

[22] Instead of the addition of $NaBH_4$/MeOH, the reaction can be quenched by passing through an alumina column to afford the product in a similar yield.

[23] NCIPLOT4; a) R. A. Boto, F. Peccati, R. Laplaza, C. Quan, A. Carbone, J.-P. Piquemal, Y. Maday, J. Contreras-García, *J. Chem. Theory Comput.* **2020**, *16*, 4150; b) J. Contreras-García, E. R. Johnson, S. Keinan, R. Chaudret, J.-P. Piquemal, D. N. Beratan, W. Yang, *J. Chem. Theory Comput.* **2011**, *7*, 625; c) E. R. Johnson, S. Keinan, P. Mori-Sánchez, J. Contreras-García, A. J. Cohen, W. Yang, *J. Am. Chem. Soc.* **2010**, *132*, 6498.

[24] F. Chen, J. Kim, Y. Matsuo, Y. Hong, D. Kim, T. Tanaka, A. Osuka, *Asian J. Org. Chem.* **2019**, *8*, 994.

[25] The aromaticity of the amine-type and imine-type pyrrole segments has been evaluated by NICS(0) and HOMA calculations (Figure S7-11).

[26] In this photoreaction, monomer **SNSN-S** is thought to be obtained via disproportion reaction of the intermediate radical species. The corresponding diradical species generated by the disproportion reaction is hydrogenated with trace amount of water in the solvent to produce **SNSN-S** (Figure S7-17). This plausible reaction mechanism is consistent with the experimental result that *β*-deuterium-labeled monomer was not obtained in the photoreaction in DMSO-d_6 in the presence of D_2O (Figure S3-24).

[27] Detailed measurement conditions: The compound **(SNSN-S)$_2$** was dissolved in THF with a concentration of 6.2 x 10^{-6} mol/L and loaded in a normal 1 cm quartz cell. Photoexcitation was carried out with continuous Hg-Xe-lamp (LC8 L9566, Hamamatsu Photonics) collimated

by a lens and an iris to a diameter of ca. 5 mm. Only 365 nm i-line was passed through a bandpass filter, and optical power was adjusted to be 600 uW. Emission spectra were simultaneously monitored by a combination of a lens, an optical fiber, spectrograph and EMCCD camera (Andor Kymera 328i and Newton 970P) with the orthogonal configuration of excitation and emission path.

[28] Without bridging units, the racemization activation energies are expected to be reduced (+31.7 kcal/mol for **SNSN-S** without a linker and +24.5 kcal/mol for **SNNN-S** without a linker), indicating the importance of closed-helicene-type structure (Figure S9-4, S9-5).

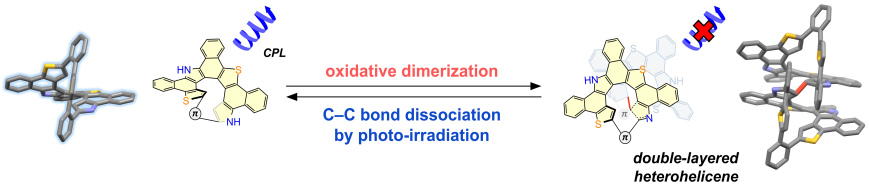

Oxidation of closed-[7]helicenes with [bis(trifluoroacetoxy)iodo]benzene gave the corresponding dimers connected at the β-positions of the pyrrole units with the remarkably elongated C–C bond about 1.60 Å. Homolytic bond dissociation took place upon UV irradiation to revert to its monomeric form. Thus, the interconversion between monomeric and dimeric forms has been achieved associated with circularly polarized luminescence (CPL) turn-ON.

Institute and/or researcher Twitter usernames: ((optional))